Neutron-scattering investigation of molecular reorientations in solid cubane

T. Yildirim
University of Maryland, College Park, Maryland 20742
and NIST Center for Neutron Research, National Institute of Standards and Technology, Gaithersburg, Maryland 20899

P. M. Gehring and D. A. Neumann
NIST Center for Neutron Research, National Institute of Standards and Technology, Gaithersburg, Maryland 20899

P. E. Eaton and T. Emrick
Department of Chemistry, University of Chicago, Chicago, Illinois 60637
(Received 29 October 1998; revised manuscript received 9 March 1999)

We have studied the reorientations of the cube-shaped molecule cubane (C_8H_8) in its solid phase using quasielastic neutron-scattering techniques both below and above the molecular orientational phase-transition temperature $T_p = 394$ K. In the orientationally ordered phase, just below T_p, the elastic incoherent structure factor (EISF) extracted from neutron time-of-flight measurements indicates that cubane undergoes π jumps about the molecular fourfold axis. In the disordered phase we find that the EISF excludes isotropic and free uniaxial rotational motions of the molecule. Instead our data suggest cubane undergoes uncorrelated π jumps about the fourfold axis (as in the ordered phase) and $2\pi/3$ jumps about the threefold axis.
[S0163-1829(99)04725-6]

I. INTRODUCTION

Molecular solids are an intriguing class of materials[1,2] in which molecules, rather than individual atoms, make up the underlying lattice. Because molecules possess rotational degrees of freedom that single atoms do not, molecular solids can exhibit molecular orientational phase transitions. At sufficiently high temperatures the molecules in such a system can enter into a phase where they begin to rotate about one or more axes, instead of librating about a fixed angular orientation as they do at low temperatures. This type of phase, in which the molecules are tumbling, is often referred to as a *plastic* phase.[2] There is a substantial interest in elucidating the solid-state properties of molecular solids that exhibit plastic phases as a function of the molecular symmetry, dynamics, and interactions. For example, solid C_{60} is a solid composed of nearly spherical molecules that exhibits a first-order orientational phase transition precisely because the C_{60} molecular symmetry deviates slightly from that of a sphere.[3] In this paper we present data from a neutron-scattering investigation of solid cubane, C_8H_8,[4] a molecular solid that is composed of remarkable cube-shaped molecules (see Fig. 1).

The molecular skeleton of cubane is extremely rigid because the C–C–C bond angle is 90° instead of the usual 109.5°. Thus cubane possesses a great deal of strain energy, about 150 kcal/mol or 6.5 eV/molecule.[6] Equally remarkable is the fact that cubane forms a stable solid at room temperature, whereas most hydrocarbons of similar molecular weight are liquids. Indeed, the unique molecular symmetry of cubane gives the solid many unusual electronic, structural, and dynamical properties.[7–12] Due to the fact that hydrogen atoms possess an exceedingly large scattering cross section for neutrons, and given the intriguing shape of the cubane molecule, solid cubane represents an ideal system with which to advance our understanding of orientational dynamics and phase transitions in molecular solids using neutron-scattering techniques.

Solid cubane adopts a rhombohedral structure with a rhombohedral angle $\alpha = 72.7°$ below $T_p = 394$ K. [Note that a face-centered-cubic (fcc) structure can also be described by a rhombohedral unit cell with a rhombohedral angle $\alpha = 60°$.[12,13]] At $T = T_p$ the solid undergoes a strongly first-order structural phase transition to a different solid phase.[9,10,12] Although many studies, including those based on Raman scattering,[10] adiabatic, and differential-scanning calorimetry (DSC),[9] and NMR measurements,[9,11] have all shown evidence of this transition at T_p, the structure of the high-temperature ($T > T_p$) phase was only recently identified using x-ray-diffraction techniques.[12] It was found that this

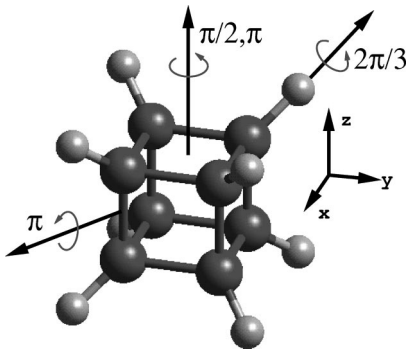

FIG. 1. Cubane in its standard orientation. Two-, three-, and fourfold rotational axes of the molecule are also shown. The large dark spheres represent carbon atoms, while the small gray spheres represent hydrogen atoms. In the standard orientation, the hydrogen atoms occupy the positions (x,x,x), $(-x,x,x)$, . . . , where $x = 1.414$ Å. The C and H positions can be determined using the bond lengths C-C=1.5618 Å and C-H=1.096 Å (Ref. 5) while assuming cubic (O_h) symmetry for the molecule.

phase is also rhombohedral, but that α has a much larger value of 103.3°. This finding was unexpected because most of the high-temperature phases of molecular solids composed of high-symmetry molecules (such as C_{60}) are fcc. The high-temperature phase of cubane persists up to $T=405$ K, at which point the solid melts.

The temperature dependence of the solid-state properties of cubane are also unusual.[12] The lattice exhibits an enormous thermal expansion of 5% between 77 K and T_p. Model calculations suggest that this is due to the presence of large amplitude rotations of the cubane molecule.[12] NMR experiments indicate that, even at room temperature (100 K below T_p), the cubane molecules are undergoing reorientational motions on a time scale of 10^{-7} sec with an activation energy of 60 meV.[11]

We have studied the molecular reorientations in solid cubane by measuring the incoherent quasielastic neutron scattering (IQNS) using neutron time-of-flight (TOF) techniques. The IQNS contains detailed information about the geometry of the reorientational jumps of the molecule that enables us to describe how these jumps occur. Raman scattering[10] and DSC (Ref. 9) methods have also been used to study the reorientational dynamics of cubane. However, these techniques can provide only limited details about the nature of the reorientational jumps. We first outline some of the basic features of incoherent neutron scattering from hydrogenous compounds (see for example Beé[14] and Lovesey[15]), and then we introduce the elastic incoherent structure factor (EISF), a fundamental quantity directly related to the average spatial distribution of the protons.

The scattering of neutrons from hydrogenous systems is strongly dominated by the incoherent scattering cross section of hydrogen (i.e., protons). In the case of cubane, the ratio of the incoherent scattering cross section of hydrogen to the *total* cross section (coherent+incoherent+absorption) of carbon is $\sigma_{inc}(H)/\sigma_t(C)=14.4$. Therefore the experimentally observed quantity is very well approximated by the incoherent scattering function $S_{inc}(Q,\omega)$ due to the hydrogen atoms alone, which is the Fourier transform of the space-time self-correlation function for the proton motions.[14,15] Here $\hbar\omega$ and Q are the energy transfer and the momentum transfer, respectively, resulting from the neutron-scattering process. Our goal is to determine the geometry and energetics of the rotational motions of the cubane molecule from an experimental measurement of $S_{inc}(Q,\omega)$.

Neutrons scattered from a molecular solid will contain information about the translational and rotational motions of the molecules (lattice modes), and about the vibrational motions of the individual nuclei within the molecules (intramolecular modes). The energies associated with the intramolecular vibrations are often much higher than those of the lattice modes, and so the two may be treated separately. This is especially true of cubane because of the extreme rigidity of the molecular skeleton. For example, at room temperature the lowest-lying internal mode of vibration is at 617 cm^{-1} (76.6 meV) whereas the highest lattice mode energy is ~ 95 cm^{-1}, a factor of 6 less in energy. A further simplication can be made by ignoring translational-rotational coupling. Although this coupling is higher in solid cubane than in most other molecular solids (cubane is very dense, 1.29 g/cm^3), this coupling is weak because the length scales associated with molecular vibrations (~ 0.1 Å) are much less than those associated with rotational jumps (~ 2 Å). We also neglect diffusion of the cubane molecule between neighboring lattice sites (self-diffusion) because the corresponding time scales are so slow that the associated quasielastic broadening cannot be observed within the experimental resolution. We may therefore interpret the experimental TOF data in terms of only the molecular rotational motions.

Within the above approximations, the observed scattering spectrum can be described by the following scattering function convoluted with the instrumental resolution function:

$$S_{inc}(Q,\omega)=e^{-2W}[A_0(Q)\,\delta(\omega)+S_{inc}^{qel}(Q,\omega)] + S_{inc}^{M}(Q,\omega)+S_{inc}^{I}(Q,\omega). \quad (1)$$

The quantity $A_0(Q)\,\delta(\omega)$ represents the purely elastic part of the scattering function, while $S_{inc}^{qel}(Q,\omega)$ represents the quasielastic part which is a measure of the Doppler broadening of the elastic line due to the rotation of the protons about the molecular center of mass. The analytic form of $S_{inc}^{qel}(Q,\omega)$ depends on the model used to describe these rotations (see the Appendix for detail). On the other hand, $A_0(Q)$, commonly called the elastic incoherent structure factor (EISF), provides a measure of the time-averaged spatial distribution of the protons, and completely characterizes the geometry of the rotational motion. For instance, for a jump motion between three and four equivalent sites, $A_0(Q)$ is an oscillatory function of Q which approaches 1/3 and 1/4, respectively, at large values of Q. In Eq. (1) the attenuation in the quasielastic region caused by vibrational motions of the molecule is taken into account by the Debye-Waller factor e^{-2W}. $S_{inc}^{I}(Q,\omega)$ is the inelastic term which contributes little to the scattering in the quasielastic region, and therefore will be treated as a small background term in the data analysis. $S_{inc}^{M}(Q,\omega)$ is the multiple-scattering contribution which, in our case, can be neglected because of the sample geometry as discussed below.

II. EXPERIMENT

All of the neutron-scattering measurements were done using the time-of-flight (TOF) Fermi-chopper spectrometer (FCS) located on neutron guide NG-6 at the National Institute of Standards and Technology Center for Neutron Research.[16] The measurements were done over a temperature range from 300–400 K, with two values of incoming neutron wavelength, namely 4.8 and 6 Å. The 0.5 g sample of microcrystalline cubane was prepared at the University of Chicago.[4] The sample was sealed inside a flat rectangular aluminum sample holder with internal horizontal and vertical dimensions of 33 and 57 mm, respectively, which were chosen to roughly match the size of the incident neutron beam with the holder oriented at a 45° angle to the beam direction. The cubane sample thickness was limited to 0.2 mm because of the large total neutron-scattering cross section of hydrogen. Furthermore, such a small sample thickness is advantageous because multiple-scattering events are minimized.

Figure 2 shows the experimental setup. The flat sample was oriented so that neutrons were scattered into the Q range ($0-0.6$ $Å^{-1}$) via transmission and ($1-2$ $Å^{-1}$) via reflec-

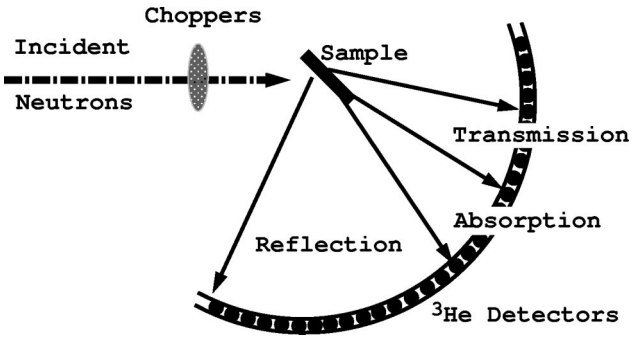

FIG. 2. Schematic diagram of the time-of-flight (TOF) Fermi-chopper spectrometer (FCS) and the sample geometry.

tion. Neutrons that are scattered along the length of the flat sample holder suffer nearly complete absorption. This effectively blocks out the Q range (0.6–1Å^{-1}). From Fig. 2 one can also see that the scattered neutrons are detected at a constant angle rather than at constant Q. This is because the momentum transfer $Q=Q(\theta,\omega)$ is a function of the scattering angle θ and of the energy transfer $\hbar\omega$. The time-of-flight technique provides a measurement of $S_{inc}(\theta,\omega)$, where Q varies as a function of $\hbar\omega$ for each detector at constant angle according to

$$Q=\left(\frac{2m}{\hbar}\{2E_0+\hbar\omega-2[E_0(E_0+\hbar\omega)]^{1/2}\cos(\theta)\}\right)^{1/2}. \tag{2}$$

In many analyses, Q is taken to be constant at its elastic value in the quasielastic region. Although this is a good approximation, we actually fit the quantity $S_{inc}(\theta,\omega)$ for each detector rather than $S_{inc}(Q,\omega)$ to scattering functions of various reorientational jump models.

Typical examples of time-of-flight IQNS spectra at room temperature and just above and below the orientational phase transition are shown in Fig. 3. At room temperature, the neutron spectrum measured at 4.8 Å can be fit to a Gaussian function (the instrumental resolution function), indicating no evidence of any spectral broadening. This is true even when using an incident neutron wavelength of 6 Å, which results in a much sharper energy resolution of 0.063 meV full width at half maximum (FWHM) (but a correspondingly lower neutron flux). This implies that the time scale of the dynamics at room temperature is slower than about 10^{-11} sec.

The spectral broadening becomes apparent close to the orientational phase transition temperature, as shown in the bottom panel of Fig. 3. Here the spectra are readily separated into elastic and quasielastic parts, the latter of which was fit to a Lorentzian function convoluted with the experimental resolution function. With only a 14 K increase in temperature from 385–399 K, the FWHM of the Lorentzian component increases from 0.34–0.57 meV, consistent with the observed orientational phase transition at $T=394$ K.

III. EXPERIMENTAL DETERMINATION OF THE EISF AND MODEL CALCULATIONS

To obtain information about the geometry of the reorientational molecular motions of cubane, we need to extract the EISF as a function of Q from the experimental data. This

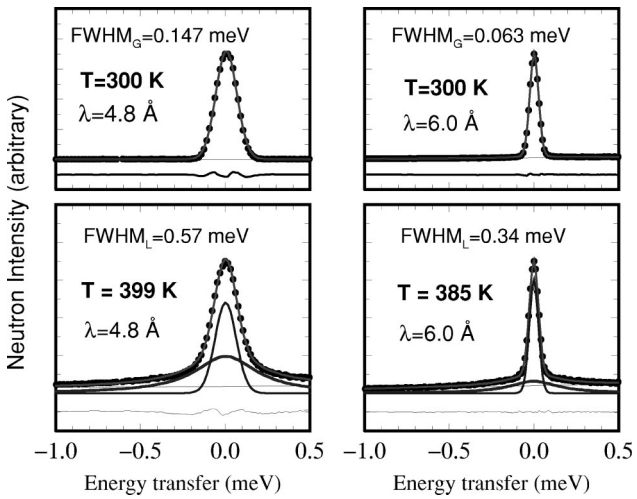

FIG. 3. Incoherent quasielastic neutron-scattering (IQNS) data (dots), fit (solid lines), and difference curve (horizontal line at the bottom) at various temperatures using two different incident neutron wavelengths. At room temperature there is no evidence of any broadening of the elastic line. In the two bottom panels, just above and below the orientational phase-transition temperature, the Lorentzian component of the scattering is clearly visible.

amounts to separating the observed spectrum for each detector at constant scattering angle θ into elastic and quasielastic components. This is most often done by fitting the experimental data to a weighted sum of two functions, one a Gaussian function to describe the elastic scattering (like that shown in the top panel of Fig. 3), and the other a Lorentzian function (which must be convoluted with the experimental resolution function) to describe the quasielastic scattering.[14] This procedure is particularly prone to uncertainties for those reorientational models that require more than just one Lorentzian function to describe the quasielastic scattering. Hence, we extracted the EISF using the equation

$$S_{inc}^{Exp}(Q,\omega)=qS_{el}(Q,\omega)+(1-q)S_{qel}^{M}(Q,\omega), \tag{3}$$

where $S_{inc}^{Exp}(Q,\omega)$ is the experimentally observed spectrum, $S_{el}(Q,\omega)$ is a Gaussian function representing the elastic resolution function, and $S_{qel}^{M}(Q,\omega)$ is the quasielastic component (not necessarily a single Lorentzian) based on a given model M. q is a fitting parameter that is used to vary the relative weighting of the two components. The experimental EISF (after fitting) is then simply q. This method of extracting the EISF from experimental data has already been used successfully by other groups.[18–20]

A. The EISF in the orientationally ordered phase

We studied the dynamics of solid cubane just below the orientational phase-transition temperature at $T=385$ K. The best fit to the data is obtained when the quasielastic component of $S_{inc}(Q,\omega)$ is approximated by a single Lorentzian function with a Q-independent linewidth. The resulting EISF and the linewidth of the Lorentzian are shown as a function of Q in Fig. 4. The thick shaded line is a guide to the eye and represents the uncertainties associated with the experimentally measured EISF.

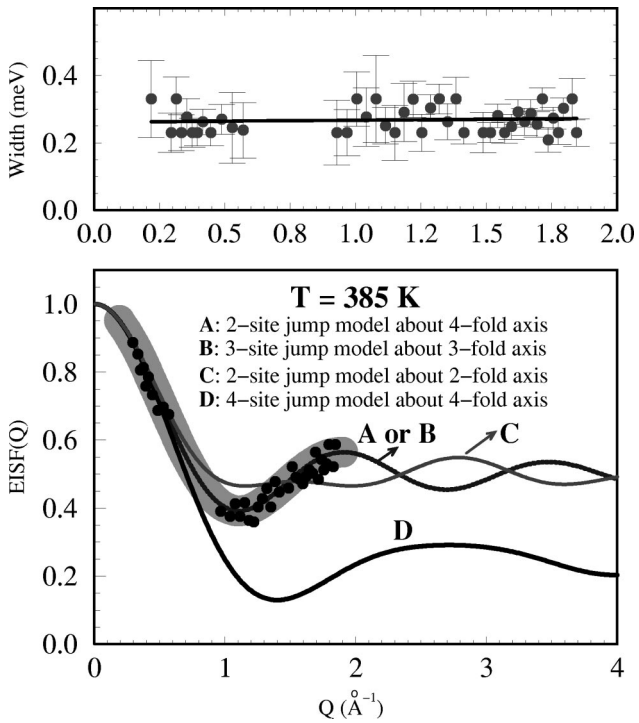

FIG. 4. Top: Linewidth of the Lorentzian component of the scattering function versus Q. Bottom: Elastic incoherent structure factors (EISF) for various jump models (solid lines) and experimental data (circles) in the orientationally ordered phase at $T=385$ K. The gap in the data between about 0.6 and 1 Å^{-1} is due to the absorption of neutrons that are scattered along the edge of the sample holder, as shown schematically in Fig. 2. The heavy gray line is a guide to the eye and indicates an upper bound on the uncertainties in the EISF vs Q.

The dynamics of most molecular solids primarily involve rotational jumps of the molecules about high symmetry axes, and so attempts to fit the data were made using rotational jump models of the cubane molecule about each of its principal axes as shown in Fig. 1. In each case the protons are assumed to undergo librational motion during an average time τ after which they jump within a set of preferred orientations. The jumps are considered to be instantaneous. X-ray data in the orientationally ordered phase[12] of solid cubane indicate a well-defined preferred orientation for the cubane molecule without any defect orientations. Hence we only consider rotational jump models that take the cubane molecule into an identical orientation.

Consider the general case of a scatterer that jumps among N equivalent sites distributed on a circle of radius r. The incoherent-scattering function for this model is given by[14]

$$S_{inc}(Q,\omega)=A_0(Q)\,\delta(\omega)+\sum_{l=1}^{N-1} A_l(Q)\,\frac{1}{\pi}\,\frac{\tau_l}{1+\omega^2\tau_l}, \quad (4)$$

where

$$A_l(Q)=\frac{1}{N}\sum_{n=1}^{N} j_0(Qr_n)\cos\left(\frac{2ln\pi}{N}\right). \quad (5)$$

TABLE I. Elastic incoherent structure factor (EISF) and correlation times (τ) for various rotational jump models for cubane. Here $x=1.414$ Å (see Fig. 1).

Models	EISF $[A_0(Q)]$	Width (τ_l)
two-site jump about twofold axis ($\phi=\pi$)	$\frac{1}{4}[2+j_0(2Qx)+j_0(2\sqrt{3}Qx)]$	$1/\tau_1=2/\tau$
two-site jump about fourfold axis ($\phi=\pi$)	$\frac{1}{2}[1+j_0(2\sqrt{2}Qx)]$	$1/\tau_1=2/\tau$
three-site jump about threefold axis ($\phi=2\pi/3$)	$\frac{1}{2}[1+j_0(2\sqrt{2}Qx)]$	$1/\tau_1=1.5/\tau$ $1/\tau_2=1.5/\tau$
four-site jump about fourfold axis ($\phi=\pi/2$)	$\frac{1}{4}[1+2j_0(2Qx)+j_0(2\sqrt{2}Qx)]$	$1/\tau_1=1/\tau$ $1/\tau_2=2/\tau$ $1/\tau_3=1/\tau$

Here j_0 is the zeroth-order spherical Bessel function. The r_n are the jump distances traveled under the effect of $(2n\pi/N)$ rotations, and are given by

$$r_n=2r\sin\left(\frac{n\pi}{N}\right). \quad (6)$$

The inverse correlation times (the Lorentzian linewidths) are

$$1/\tau_l=2/\tau\sin^2\left(\frac{\pi l}{N}\right). \quad (7)$$

Using these expressions, the EISF for each of the different jump geometries for cubane can easily be derived. These are summarized in Table I. For example, rotations about the threefold axis of cubane involve 2×3 protons performing jumps among three-equivalent sites on a circle, while the other two protons do not move at all. The total EISF is therefore simply a weighted average of the respective EISF for each of these two distinct types of protons, i.e., $\frac{1}{8}[2\times\mathrm{EISF}(1)+6\times\mathrm{EISF}(3)]$, where $\mathrm{EISF}(1)=1$ and $\mathrm{EISF}(3)$ is the structure factor for three-site jumps given above. Hence in the three-site jump model, one expects one Lorentzian with a constant width, in agreement with experiment. Similarly, for two-site jumps about the two-fold axis of cubane (see Fig. 1) we also have two types of protons, each performing rotational jumps over two sites on circles of two different radii. Again, the total EISF is the weighted average of the EISF for each type of proton. Since the cubane molecule is so rigid, both types of protons must have basically the same dynamical correlation times. Hence the quasielastic part of the incoherent-scattering function for this model is also described by a single Lorentzian function with a constant width.

The solid lines in Fig. 4 show the EISF Q dependence expected for the various models listed in Table I. The experimental EISF agrees very well with that for rotational jumps of cubane about its fourfold axis by π ($N=2$), or about its threefold axis by $2\pi/3$ ($N=3$). Unfortunately the EISF's for these two models are identical (by accident), and therefore it

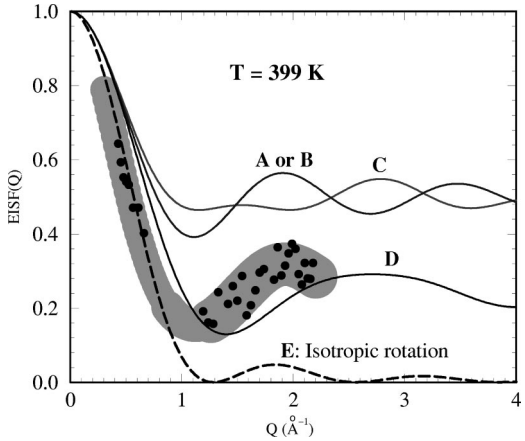

FIG. 5. Elastic incoherent structure factors (EISF) for various models (solid lines) and experimental data (circles) at $T=399$ K (in the orientationally disordered phase). The heavy gray line is a guide to the eye and indicates an upper bound on the uncertainties in EISF vs Q. Curves labeled A, B, C, and D depict the same EISF's for the reorientational jump models described in Fig. 4.

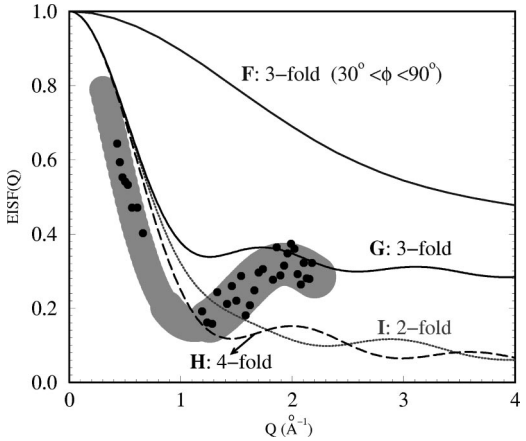

FIG. 6. Elastic incoherent structure factors (EISF) for uniaxial rotational diffusion about the principal axes of cubane molecule.

is not possible to distinguish them using IQNS alone. However, from model calculations we know that the energy barrier for the fourfold rotation is lower than that for the threefold rotation.[17,21,12] It is thus tempting to conclude that the dominant reorientational motion corresponds to jump rotations about the fourfold axis. Cubane can do this by performing either $\pi/2$ (four-site) or π (two-site) jumps. From Fig. 4, it is clear that $\pi/2$ jumps are not favorable, which is quite interesting. The reason for this is not clear. However, we note that similar behavior is also observed in other systems.[22] This probably has to do with the memory of the reorientational dynamics and kinematical reasons. It is quite possible that once a molecule jumps it is likely to perform another one instantly. Collective effects probably play an important role in this.

B. The EISF in the orientationally disordered phase

The dynamics of solid cubane were studied in the orientationally disordered phase at $T=400$ K, just 5 K below the melting point of the solid. The experimental EISF at this temperature is shown in Fig. 5. Although the EISF in both the ordered and disordered phases exhibits a minimum around $Q=1.1$ Å, the minimum value of the EISF in the disordered phase (<0.2) is less than half of that found in the ordered phase (0.4). Comparing the data to the various rotational jump models of cubane which are also shown in Fig. 5, we see that none can describe the reorientational dynamics of solid cubane in the orientationally disordered phase.

We next consider the isotropic rotational diffusion model[23] which describes, for example, the high-T dynamics of both norbornene[24] and powdered C_{60}.[25] In this model the molecules are assumed to perform more or less continuous, random small-angle rotations. This means that, over time, the protons have no preferred orientation in space. The only adjustable parameter in this model is the isotropic diffusion constant D_R. The best fit to the measured EISF for this model corresponds to curve **E** shown in Fig. 5. As all of the experimental data lie well above the curve obtained from this model for $Q>1$ Å^{-1}, we conclude that the molecules do not undergo isotropic diffusive rotations in the high-T solid phase of cubane. This conclusion is further supported by our x-ray study,[12] as well as the recent NMR study by Detken *et al.*[11]

The fact that the isotropic rotational diffusion model does not fit the experimental EISF is interesting because it provides evidence that the high-T molecular dynamics of solid cubane are anisotropic, at least over the time scales probed by the neutron TOF technique. This suggests we consider the possibility that cubane may instead undergo uniaxial diffusive molecular rotations about the principal axes shown in Fig. 1. In fact, the results of our recent x-ray study showed that the molecular orientational disorder of cubane is well described by a constant distribution of setting angles[26] between 50° and 70°.[12] In agreement with the x-ray data, our model calculations[12] indicate that the potential energy is very flat as the molecules are collectively rotated about the [111] axis from 30° to 90°, after which the potential energy increases very rapidly. These results suggest that a uniaxial rotational diffusion model that is restricted to a limited angular range about the threefold [111] axis might describe the high-temperature dynamics of solid cubane.

In Fig. 6 we show the EISF from such a rotational diffusion model (curve F). The calculations of the EISF for this model are given in the Appendix. For completeness, we also calculated the EISF for unbounded uniaxial diffusive rotations about each of the three principal axes shown in Fig. 1. The results are shown in Table II, and the EISF for each model is plotted versus Q in Fig. 6. Surprisingly, none of these models alone can describe the experimental data. It is important to note that this result is not in disagreement with the x-ray study and potential calculations since it is quite possible that the time scale of this motion lies outside that probed by our TOF neutron measurements.

Alternatively, there may be more than one type of motion controlling the EISF. If two types of motions occur independently, then the resulting EISF is simply the product of the structure factor of each individual motion. This is because the total scattering function is the convolution of the individual scattering functions. In Fig. 7 we plot the EISF (curve A*F) for the case where the molecules are performing both two-site jumps about a fourfold axis (curve A) and uniaxial

TABLE II. Elastic incoherent structure factors (EISF) for uniaxial rotational diffusion about the principal axes of the cubane molecule. Here N is a large number (≥ 50) and $x = 1.414$ Å (see Fig. 1).

Model	EISF $[A_0(Q)]$	Radius
twofold	$(1/2N)\Sigma_{i=1}^{N} j_0[2Qr_2^{(1)}\sin(\pi i/N)]$	$r_2^{(1)} = \sqrt{3}x$
	$+(1/2N)\Sigma_{i=1}^{N} j_0[2Qr_2^{(2)}\sin(\pi i/N)]$	$r_2^{(2)} = x$
threefold	$\frac{2}{8} + (6/8N)\Sigma_{i=1}^{N} j_0[2Qr_3 \sin(\pi i/N)]$	$r_3 = \sqrt{8/3}x$
fourfold	$(1/N)\Sigma_{i=1}^{N} j_0[2Qr_4 \sin(\pi i/N)]$	$r_4 = \sqrt{2}x$

rotational diffusion in a bounded angular region over a circle (curve F). Even though the calculated EISF for such a model gets closer to the experimental data at high Q, the overall agreement is not good.

We finally consider the possibility of two uncorrelated rotational jumps: one a two-site jump about a fourfold axis (curve A) and the other a three-site jump about a threefold axis (curve B). As discussed in the previous section, both models give the same EISF. In Fig. 7, we show the product curve A*B as a solid line. Clearly this gives very good agreement with the data. Considering the fact that we are very close to the melting point of the solid where the importance of self-diffusion and rotational-translational mode coupling becomes significant, the agreement between the experiment and this model seems quite convincing. It is particularly so since in the ordered phase we observe the two-site jump about a fourfold axis, and there is no reason why we should not see the same reorientation in the high-T phase. Apparently in the disordered phase the barrier for the three-site jump is low enough to allow this type of motion to occur as well.

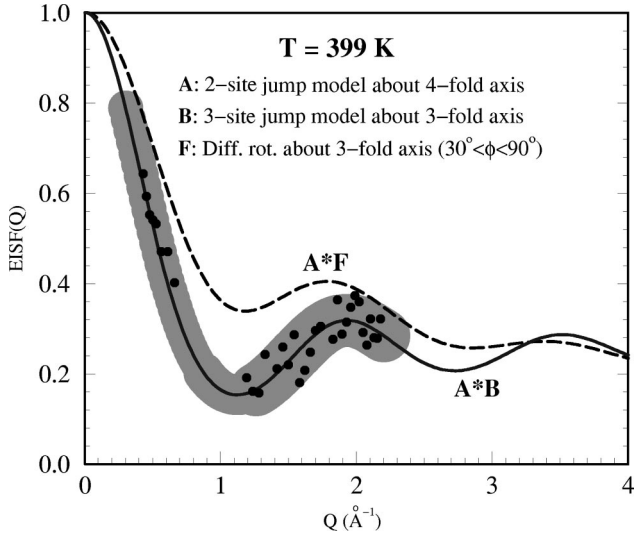

FIG. 7. Elastic incoherent structure factors (EISF) for various models (dashed and solid lines) and experimental data (circles) at $T = 399$ K (5 K above phase transition). Curves labeled by A*F and A*B are the structure factors for models involving two types of dynamics simultaneously.

A recent NMR study[11] of cubane at 400 K presented evidence of molecular self-diffusion between lattice sites with a correlation time of 10^{-6} sec. The presence of self-diffusion suggests that weak, isotropic orientational correlations govern the molecular dynamics of cubane at this temperature. Yet in spite of this, and in spite of the large changes in the volume and shape of the unit cell that take place during the first-order phase transition, the IQNS data we have presented show that the orientational dynamics of cubane are instead highly anisotropic, even at temperatures just 5 K below its melting point. This indicates that strong orientational correlations still exist between the molecules.

IV. CONCLUSION

We have studied the dynamics of solid cubane in both the orientationally ordered and disordered phases using incoherent quasielastic neutron-scattering techniques. The experimentally measured EISF in both phases were compared to a large number of models, including a variety of rotational jump and diffusion models. We can summarize our conclusions as follows:

(i) In the orientationally ordered phase, the observed EISF can be well described by simple rotational π jumps about the fourfold axis of the molecule. Rotational $2\pi/3$ jumps about the molecular threefold axis, which result in same EISF, can most likely be excluded by potential energy barrier considerations. It is interesting to note that $\pi/2$ jumps about the fourfold axis are ruled out by the data.

(ii) In the orientationally disordered phase, the observed EISF rules out single rotational-jump models, as well as isotropic and uniaxial rotational diffusion models.

(iii) In the orientationally disordered phase, the EISF was compared to a bounded uniaxial rotational diffusion model about the threefold axis as suggested by previous x-ray and model potential calculations.[12] This model did not agree with the observed data. This is most likely due to the fact that time scale of such motions occurs on a longer time scale than that probed in this study.

(iv) The best agreement to the experimental EISF in the orientationally disordered phase is obtained by assuming two types of uncorrelated rotational jumps. One of them is the same as found in the ordered phase, i.e., π jumps about the fourfold axis. The other is $2\pi/3$ jumps about the threefold axis.

(v) Since the melting point lies only 10 K above the transition to the orientationally disordered phase, one has to be concerned with other factors, such as self-diffusion and rotational-translational coupling. In order to obtain detailed information about these, one needs to perform similar IQNS studies using TOF and backscattering methods, probably on single crystals. However such single-crystal experiments are exceedingly difficult to carry out in the high-T phase. Many serious complications occur due to very high vapor pressure and rate of recrystallization of cubane. And the proximity of the disordered phase to liquid phase requires an accurate and

stable temperature control apparatus. Perhaps the only way to overcome these difficulties is to perform these experiments in a controlled environment, such as is done in state-of-the-art molecular dynamics. We are currently developing an intermolecular potential from first principles and performing such molecular-dynamics simulations. We hope that these studies will be useful in helping us to understand the many unique properties of solid cubane in particular, and in advancing our understanding of molecular solids in general.

ACKNOWLEDGMENT

T.Y. acknowledges partial support from the National Science Foundation under Grant No. INT97-31014.

APPENDIX: CALCULATION OF THE ELASTIC INCOHERENT STRUCTURE FACTOR (EISF) FOR A GENERAL MODEL

In this appendix we present a practical approach to calculate the elastic incoherent structure factor (EISF) $A_0(Q)$ for a given model of the dynamics for a single proton. We are particularly interested in calculating $A_0(Q)$ for a rotational diffusion model confined to a circle and a limited angular range $[\theta_0, \theta_f]$. X-ray measurements and potential energy calculations[12] strongly suggest such a model is relevant for solid cubane in the orientationally disordered phase.

We start with the so-called elastic incoherent structure factor (EISF), which provides information about the region of space accessible to the scatterer, i.e., about the geometry of the motion

$$A_0(\mathbf{Q}) = \langle e^{i\mathbf{Q}\cdot[\mathbf{r}_i(\infty)-\mathbf{r}_i(0)]}\rangle = \langle e^{i\mathbf{Q}\cdot\mathbf{r}_i(\infty)}\rangle\langle e^{i\mathbf{Q}\cdot\mathbf{r}_i(0)}\rangle = |\langle e^{i\mathbf{Q}\cdot\mathbf{r}_i(0)}\rangle|^2. \tag{A1}$$

The last line above follows from the fact that there is no correlation between the positions of the scatterer at $t=0$ and at an infinite time later.

From the above equation, we see that we need to know the coordinates of the positions occupied by the scatterer during the dynamics under consideration in order to calculate $A_0(\mathbf{Q})$. From now on, we will assume that any dynamical model can be described by a set of discrete sites that the scatterer visits during the dynamics. By allowing for a large number of such discrete positions, one can easily recover the dynamical models involving continuous motions. Let $\mathbf{r}_i$, $i=1,\ldots,N$, represent the position vectors that the scatterer visits with the occupancy probabilities p_i, $i=1,\ldots,N$, where $\Sigma_{i=1}^{N} p_i = 1$. Within this description the ensemble average in Eq. (A1) can be written as

$$A_0(\mathbf{Q}) = \left|\sum_{i=1}^{N} p_i e^{i\mathbf{Q}\cdot\mathbf{r}_i}\right|^2 = \sum_{i=1}^{N}\sum_{j=1}^{N} p_i p_j e^{i\mathbf{Q}\cdot(\mathbf{r}_i-\mathbf{r}_j)}. \tag{A2}$$

Next we need to perform a powder average to allow $\mathbf{Q}$ to take on all possible orientations relative to $\mathbf{r}_i$. Using the relation

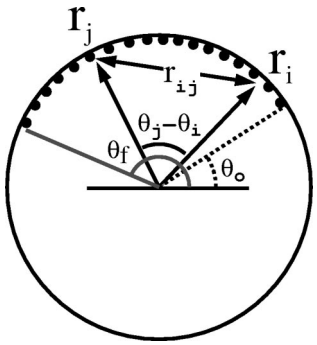

FIG. 8. Schematic representation of the N-site model on a circle with a bounded angular region over which the scatterer can jump.

$$\langle e^{i\mathbf{Q}\cdot\mathbf{R}}\rangle_{pow.av.} = j_0(QR), \tag{A3}$$

where $j_0(x)$ is the zeroth-order spherical Bessel function, we obtain

$$A_0(Q) = \langle A_0(\mathbf{Q})\rangle_{pow.av.} = \sum_{i=1}^{N}\sum_{j=1}^{N} p_i p_j j_0(Q|\mathbf{r}_i-\mathbf{r}_j|). \tag{A4}$$

This forms the master equation for calculating $A_0(Q)$ for an arbitrary model.

We apply this formula first to the model where a scatterer moves over a circle of radius r but is constrained to the angular region from θ_0 to θ_f as shown schematically in Fig. 8. From this figure, one can obtain

$$r_{ij} = |\mathbf{r}_j - \mathbf{r}_i| = 2r\sin\left|\frac{\theta_j-\theta_i}{2}\right|, \tag{A5}$$

where

$$\theta_i = \frac{\theta_f-\theta_0}{N} i. \tag{A6}$$

Thus the final expression for the EISF is

$$A_0(Q) = \frac{1}{N^2}\sum_{i=1}^{N}\sum_{j=1}^{N} j_0\left(2Qr\sin\left|\frac{\theta_f-\theta_0}{2N}(j-i)\right|\right). \tag{A7}$$

Calculating $A_0(Q)$ with various values of N larger than 50 yield results that are basically the same. Therefore $N=50$ is large enough to model continuous rotational diffusion. In Fig. 6 the resulting EISF is plotted for the parameters $\theta_f-\theta_0=60^{\circ}$ and $r=\sqrt{8/3}x\sim 4\sqrt{3}$ Å which are the appropriate values for the cubane molecule.

We can apply this master equation to the case of uniaxial rotational diffusion too. If we take $\theta_f-\theta_0=2\pi$ and perform the summation over i and $k=i-j$, one obtains

$$A_0(Q) = \frac{1}{N}\sum_{k=1}^{N} j_0\left[2Qr\sin\left(\frac{k\pi}{N}\right)\right] \tag{A8}$$

which is identical to the expression given in Eq. (5) with $l=0$. Applying this equation to a cubane molecule performing continuous rotational diffusion about its principal axes, one obtains the formulas listed in Table II, and which are plotted in Fig. 6.

[1] N. G. Parsonage and L. A. K. Staveley, *Disorder in Crystals* (Clarendon Press, Oxford, 1978); A. I. Kitaigorodsky, *Molecular Crystals and Molecules* (Academic Press, New York, 1973).
[2] K. H. Michel and K. Parlinski, Phys. Rev. B **31**, 1823 (1984); M. Yvinec and R. M. Pick, J. Phys. (France) **41**, 1045 (1980).
[3] P. A. Heiney *et al.*, Phys. Rev. Lett. **66**, 2911 (1991); R. Sachidanandam and A. B. Harris, *ibid.* **67**, 1467 (1991).
[4] P. E. Eaton and T. W. Cole, Jr., J. Am. Chem. Soc. **86**, 962 (1964).
[5] Lise Hedberg *et al.*, J. Am. Chem. Soc. **113**, 1514 (1991).
[6] B. D. Kybett, S. Carroll, P. Natallis, D. W. Bonnell, J. L. Margrave, and J. L. Franklin, J. Am. Chem. Soc. **88**, 626 (1966); S. Borman, Chem. Eng. News **72**, 34 (1994).
[7] V. Galasso, Chem. Phys. **184**, 107 (1994).
[8] P. M. Gehring *et al.*, J. Phys. Chem. **99**, 4429 (1995).
[9] M. A. White *et al.*, J. Phys. Chem. **96**, 421 (1992).
[10] R. A. Dalterio and F. J. Owens, Solid State Commun. **67**, 673 (1988).
[11] A. Detken *et al.*, J. Phys. Chem. **100**, 9598 (1996).
[12] T. Yildirim, P. M. Gehring, D. A. Neumann, P. E. Eaton, and T. Emrick, Phys. Rev. Lett. **78**, 4938 (1997).
[13] E. B. Fleischer, J. Am. Chem. Soc. **86**, 3889 (1964).
[14] M. Beé, *Quasielastic Neutron Scattering* (IOP Publishing Ldt., Bristol, 1988).
[15] For example, see S. Lovesey, *Theory of Neutron Scattering from Condensed Matter*, 3rd ed. (Oxford University Press, New York, 1987).
[16] J. R. D. Copley and T. J. Udovic, J. Res. Natl. Inst. Stand. Technol. **98**, 71 (1993).
[17] T. Yildirim *et al.* (unpublished).
[18] R. E. Lechner, J. P. Amoureux, M. Beé, and R. Fouret, Commun. Phys. **2**, 207 (1977).
[19] M. Beé and J. P. Amoureux, Mol. Phys. **50**, 585 (1983).
[20] M. Beé, J. L. Sauvajol, and J. P. Amoureux, J. Phys. (France) **43**, 1797 (1982).
[21] C. A. Fyfe and D. J. Harold-Simith, J. Chem. Soc., Faraday Trans. 2 **71**, 967 (1975).
[22] R. W. Gerling and A. Hüller, J. Chem. Phys. **78**, 446 (1983).
[23] V. F. Sears, Can. J. Phys. **44**, 1299 (1966); **45**, 234 (1967).
[24] M. Beé, H. Jobic, and C. Caucheteux, J. Chim. Phys. Phys.-Chim. Biol. **83**, 10 (1986).
[25] D. A. Neumann *et al.*, Phys. Rev. Lett. **67**, 3808 (1991).
[26] The setting angle refers to the collective rotation of molecules around the crystallographic [111] axis. A zero setting angle corresponds to the standard orientation of cubane shown in Fig. 1.